S0032-3861(96)00890-7

Castor oil-based polyurethanes: 2. Tridimensional polyaddition in bulk between castor oil and diisocyanates—gelation and determination of F_w(OH)

Ngoc Buu Tran
Centre de Service d'Analyse et d'Expérimentation, 2 Nguyen Van Thu, Q. 1, Hô chi Minh-Ville, Vietnam

and Quang Tho Pham*
CNRS—Service Central d'Analyse et URA 507, BP 22, F-69390, Vernaison, France
(Received 24 June 1996; revised 16 September 1996)

Quantitative liquid ^{13}C-n.m.r. has been extensively employed for the study of swollen gels. In the bulk tridimensional polyadditions of pure triricinoleate of glycerol (R_3G) and castor oil (CO) with 4,4'-methylenediphenylisocyanate, 2,6-tolylene diisocyanate and 1,6-hexamethylene diisocyanate, the conversions of alcohol and of isocyanate groups were found to be limited by the crosslink density of the networks. The conversion limits were found independent of the natures of the diisocyanates incorporated. Critical times at the sol–gel transitions were localized by dynamic mechanical experiments. The conversion limits of OH groups determined in dense gels are only slightly larger than those found at critical times. Thanks to the conversion limits of dense gels and the known values of the R_3Gs and COs weight-average functionalities of OH groups [$\overline{F_w}$(OH)], a reliable graphical method has been established for the determination of $\overline{F_w}$(OH) usable for other reactive prepolymers. © 1997 Elsevier Science Ltd.

INTRODUCTION

During the past few decades, castor oil (CO)—a low cost natural vegetable oil bearing hydroxyl groups—has been used to replace expensive synthetic polyols in industrial production of cross-linked polyurethanes[2–4] and/or interpenetrated polymer networks (IPN)[5,6] having low glass transition temperature and high impact-resistance. In almost all the published works, studies were generally focused on physical and/or mechanical properties of the materials obtained.

With a number-average hydroxyl functionality ($\overline{F_n}$(OH)) of 2.7[1,4], the tridimensional polycondensation in bulk of CO with diisocyanates already gives microgels at hydroxyl conversion of 30%. Because of the cross-linking, chemical analyses of the remaining OH and/or NCO groups are inoperative, particularly at and beyond the gel points (GP). Thus the critical conversion (p_c) at which the weight-average molecular weight ($\overline{M_w}$) becomes infinite-related to the weight-average hydroxyl functionality [$\overline{F_w}$(OH)][7,8] remain an open question.

In our preceding paper[1], a quantitative study of the seven CO intact glyceride fractions separated by semi-preparative liquid chromatography (l.c.) was achieved by using fatty acids methyl ester-gas chromatography (FAME-g.c.) and mass spectrometry (m.s.). CO was found principally constituted of 70% of triricinoleate of glycerol (R_3G, triol) and 30% of diricinoleate-mono (non-hydroxylated)acyl (X) glycerols (R_2XG, diols), thus the possible calculations of $\overline{F_w}$(OH) (= 2.8) and I_p (OH) [= $\overline{F_w}$(OH)/$\overline{F_n}$(OH) = 1.03]. With these known values, the present work deals with the establishment of the optimal conditions needed for the graphical determinations of the R_3G and CO $\overline{F_w}$(OH)s taking into account the variation of p_c values of the gels determined by quantitative ^{13}C n.m.r. against NCO/OH ratios. The results may be checked by solvent swelling experiments. The method should easily be generalized for the determination of the F_w of other prepolymers' reactive end-groups, for example the radically obtained hydroxytelechelic polybutadienes (HTPB)[9].

EXPERIMENTAL

Reagents

Castor oil (CO—Aldrich Chemie, Fallavier, France) and pure triricinoleate of glycerol (R_3G) extracted from CO by flash chromatography[1] were vacuum dried before use. High purity, solid 4,4'-methylene di(phenylisocyanate) (MDI-Bayer, France, Ag, 98%), 2,6-tolylene diisocyanate (2,6-TDI—Fluka, Fallavier, France, 97%) and 1,6-hexamethylene diisocyanate (HMDI—Fluka, 98%) were stored under dry nitrogen atmosphere before use.
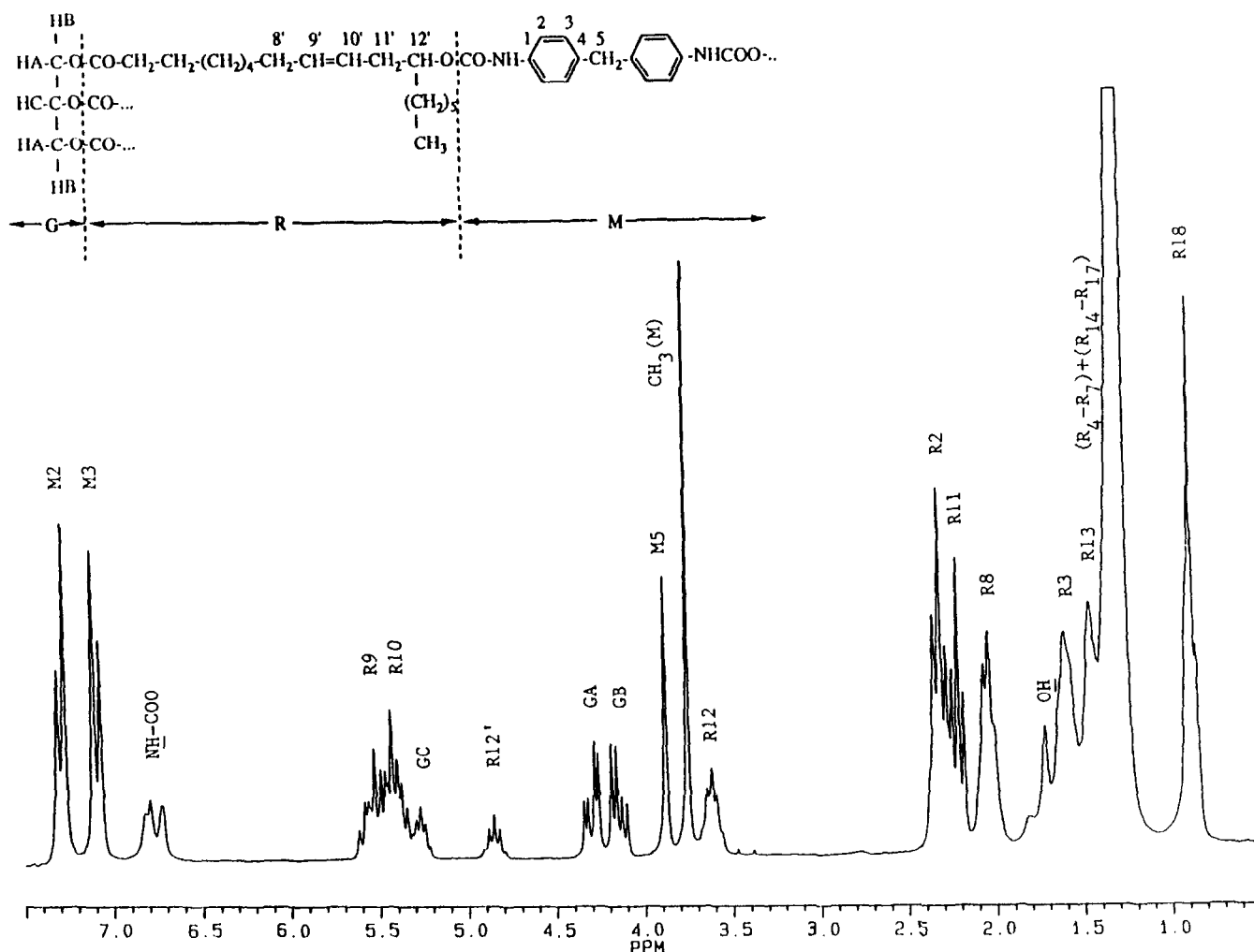

Figure 1 ^{1}H (200 MHz) n.m.r. spectrum of a soluble castor oil-based polyurethane obtained in bulk with the mixture $(R_3G + MDI)$ (NCO/OH = 0.8). Conversion of OH = 27%. Solvent: C_6D_6, room temperature

Bulk polycondensations

Because MDI melts at 42°C polyadditions in bulk—at temperatures equal to 40°C or higher—were performed in a thermoregulated reactor under nitrogen atmosphere with different NCO/OH ratios (r). For good homogenization, solid MDI was powdered before use. Non-reacted NCO groups remaining in gels or in (sol + gel) mixtures were destroyed by an excess of cold methanol under ultrasonic agitation. The actual presence of gels or microgels (clusters) was verified by dissolution in toluene with ultrasonic agitation during several hours. In toluene, with increasing conversions, the CO-based polyurethane (CO-PU) samples may be totally soluble, partially soluble (sol with microgels or clusters), or totally insoluble (dense gel). Before n.m.r. examinations, toluene and methanol in excess were eliminated by vacuum.

^1H and ^{13}C-n.m.r. spectrometry

Samples of CO-based polyurethanes (CO-PU) were dissolved or swollen in C_6D_6 under ultrasonic agitation. ^{1}H and ^{13}C-n.m.r. spectra were recorded at room temperature using a Bruker AC 200 spectrometer (200 MHz and 50.3 MHz for ^{1}H and ^{13}C respectively). The destruction of non-reacted NCO groups in CO-PU by methanol (with the methoxy lines at 3.5 and 50 ppm for ^{1}H and ^{13}C respectively) gives methyl carbamate

ends (with the methoxy lines at 3.75 and 52 ppm for ^{1}H and ^{13}C respectively, *Figures 1* and *2*)
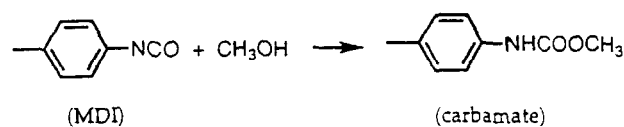
Typical analysis conditions were:

^{1}H-n.m.r. Concentration of soluble CO-PU = 5% (w/v) in C_6D_6; pulse angle = 13°; acquisition time = 3.9 s for 16 k-words; sweep width = 2994 Hz; repetition time = 5.9 s; number of scans = 2000.

^{13}C-n.m.r. Concentration of insoluble CO-PU swollen in $C_6D_6 = 40\%$ (w/v); n.m.r. tube diameter = 5 mm; pulse angle = 40°; acquisition time = 1.4 s for 32 k-words; sweep width = 11 627 Hz; repetition time = 21.4 s; number of scans = 10 000; these analysis conditions permit quantitative determinations without addition of any relaxation reagent affecting spectral resolution.

Dynamic mechanical measurements

Dynamic mechanical measurements were performed using a Rheometrics Dynamical Analyser RDA 700. The
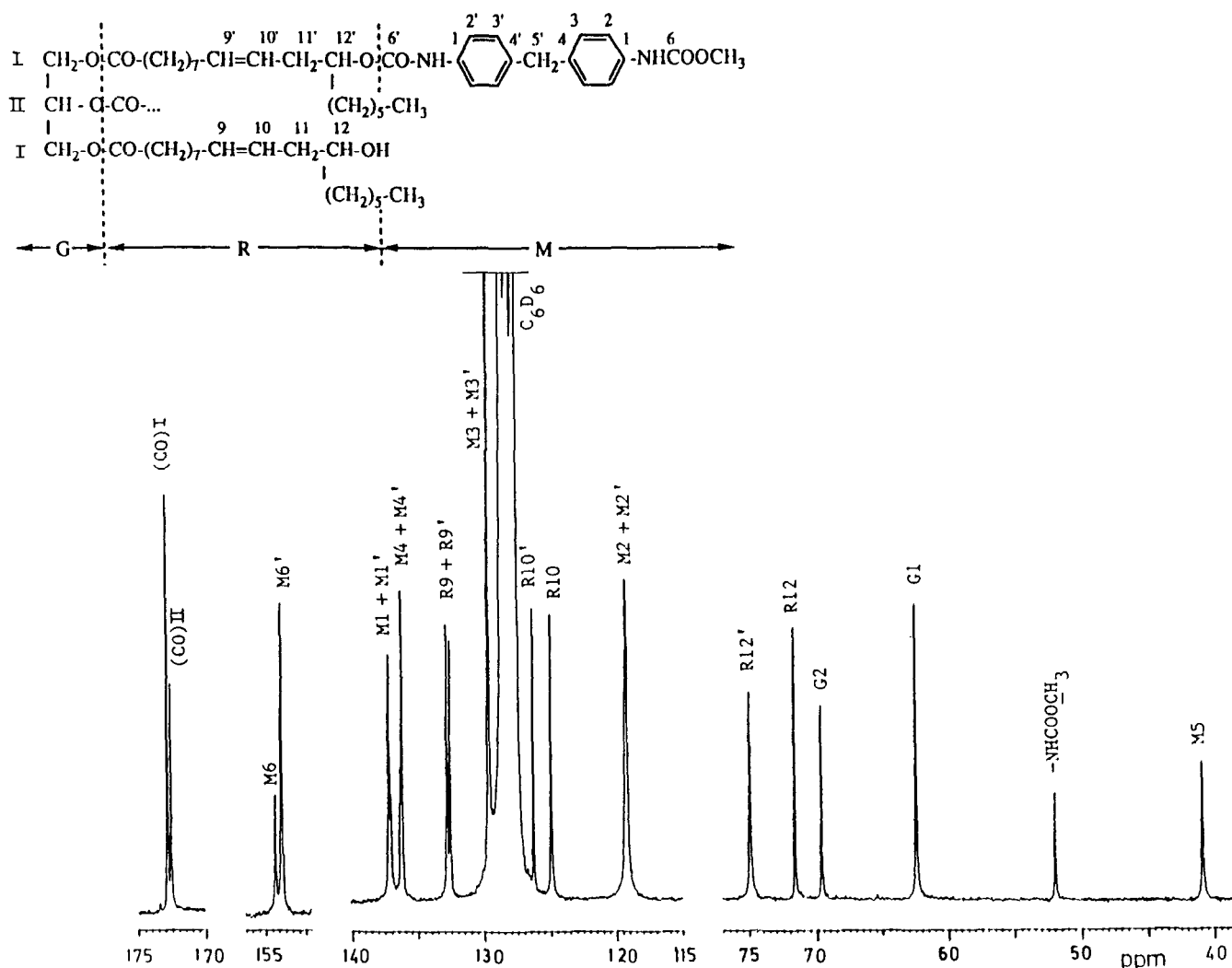
Figure 2 ^{13}C (50.3 MHz) n.m.r. spectrum of a swollen castor oil-based polyurethane gel obtained in bulk with the mixture ($R_3G + MDI$) (NCO/OH = 0.8). Conversion of OH = 51%, swelling solvent: C_6D_6, room temperature. The (13–38 ppm) region is not shown

reactive mixture was placed between the 20 mm-diameter parallel disks of the rheometer. At regular time intervals, the reactions were examined in the frequency sweep mode in the $1-100 \, \text{rad s}^{-1}$ region at 50°C.
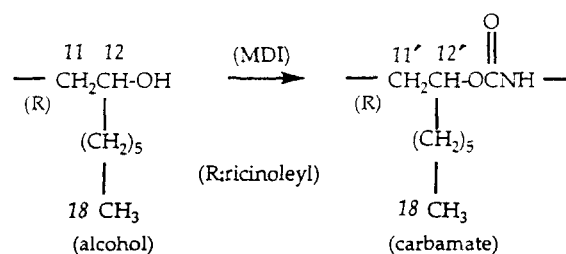
Equilibrium swelling

The equilibrium swelling Q_m is defined as the ratio of the volume of the swollen gel over the volume of the dry extracted gel[14,15,17]. The extraction was performed in methylcyclohexane at 295 K, and Q_m measured at the end of the extraction. The extrapolation to the maximum value of Q_m ($Q_m^{-1} \to 0$) give the minimum value of NCO/OH ratio, its critical or threshold value (r_t) allowing gelation, and thus another possible extrapolation permitting the calculation of $\overline{F_w}(OH)$.

RESULTS AND DISCUSSION

Because of the unique nature its three acyls, triricinoleate of glycerol (R_3G)—having the same three secondary alcohols borne by the three carbons ^{12}C (*Scheme 1*)—may be considered as a model. Moreover, each hydroxyl being far (26 carbons + 2 oxygens) from the other should react independently. In other words, the reactivity of the alcohol functions should remain constant, at least before the threshold of cross-linking induced steric hindrance.

For low conversion (<30%), CO-PUs are soluble. The typical H^1-n.m.r. spectrum of a soluble CO-PU given by the ($R_3G + MDI$) mixture with $r = \text{NCO/OH} = 0.8$ is illustrated in *Figure 1*. The conversion [$p(OH)$] of the secondary alcohol in carbamate is easily determined by comparing the relative intensities of the corresponding methine protons: R12 (alcohol, quintet) at 3.6 ppm and R12′ (carbamate, quintet) at 4.85 ppm [*Scheme 1*, equation (1)]

$$p(OH) = \frac{(R12')}{(R12) + (R12')} \times 10^2 \qquad (1)$$

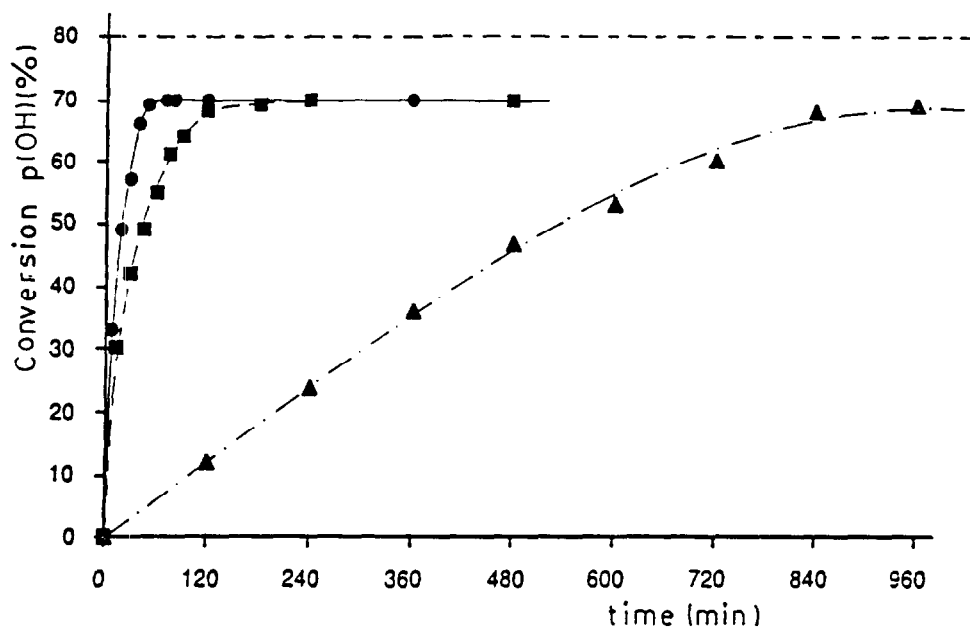(R12), (R12′) are the relative intensities of the corresponding protons.

Thus for soluble CO-PUs, quantitative determinations of the conversions may be rapidly achieved by ^{1}H n.m.r. But unfortunately since 30% of conversion ^{1}H n.m.r. becomes unserviceable because of the presence

Triol = triricinoleate of glycerol ($R_3G = 70$ %)

HB
|
HA— C$_I$O — R
|
HC— C$_{II}$O — R
| 9   12   18
HB— C$_I$O — CCH$_2$(CH$_2$)$_6$CH=CHCH$_2$CHCH$_2$(CH$_2$)$_4$CH$_3$
| || |
HB   O   OH

(G)   (R)

Diols = diricinoleate-monoacyl (X) of glycerol ($R_2XG = 30$ %)

CH$_2$O - R   CH$_2$O - R
| |
CHO - R   or   CHO - X
| |
CH$_2$O - X   CH$_2$O - R

X (non-hydroxylated acyl) = linoleyl , linolenyl , oleyl ,...

Scheme 1

of microgels, only quantitative liquid ^{13}C n.m.r. (more time consuming) may be utilized because gelled CO-PUs are easily swollen by benzene.

Figure 2 shows the well-resolved ^{13}C n.m.r. spectrum of a homogeneously swollen CO-PU (sol + gel) obtained at 51% of OH conversion. Again, the same equation (1) may be applied with (R12) and (R12′) being now the relative intensities of the corresponding carbons. It is instructive to note that

(a) methanol is efficient for destroying remaining NCO functions giving methyl carbamate that splits almost all the MDIs carbon resonance lines, except M3 (129.5 ppm) and M5 (41 ppm);

(b) the effects of the carbamate group borne by carbon 12 (R12′) are even felt beyond the double bond by carbon 9 (R9 and R9′ at around 133 ppm).

All these splittings allow the cross-checks of the conversions given by R12 and R12′.

Effects of the reaction temperature

From the three polyadditions in bulk of (R_3G + MDI) with r = NCO/OH = 0.8 at 40, 50 and 60°C (*Figure 3*), the common point is the limit of 70% of the OH conversions. In other words, even with OH in excess, the conversion of NCO [p(NCO)] is incomplete.

$$p(NCO) = p(OH) : r \quad \text{(with } r = 0.8 < 1) \quad (2)$$

with p(OH) = 70%, p(NCO) = 87.5%.

In all cases, the conversions of the mixtures were determined by comparing R12- and R12′-methine C13 resonances [equation (1)].

Because of gelation, a proportion of the NCO reactive ends should be trapped in the CO-PU networks. The

Figure 3 Polyadditions in bulk of (R_3G + MDI) with r = NCO/OH = 0.8. Conversions p(OH)% = f (time) at 40°C (▲), 50°C (■) and 60°C (●). (————): theoretical conversion limit = 80%

Figure 4 Polyadditions in bulk of (R_3G + diisocyanate) with r = NCO/OH = 0.8 at 50°C. Conversions p(OH)% = f (time). (●) MDI; (■) 2,6-TDI; (▲) HMDI; (– – – –) theoretical conversion limit = 80%

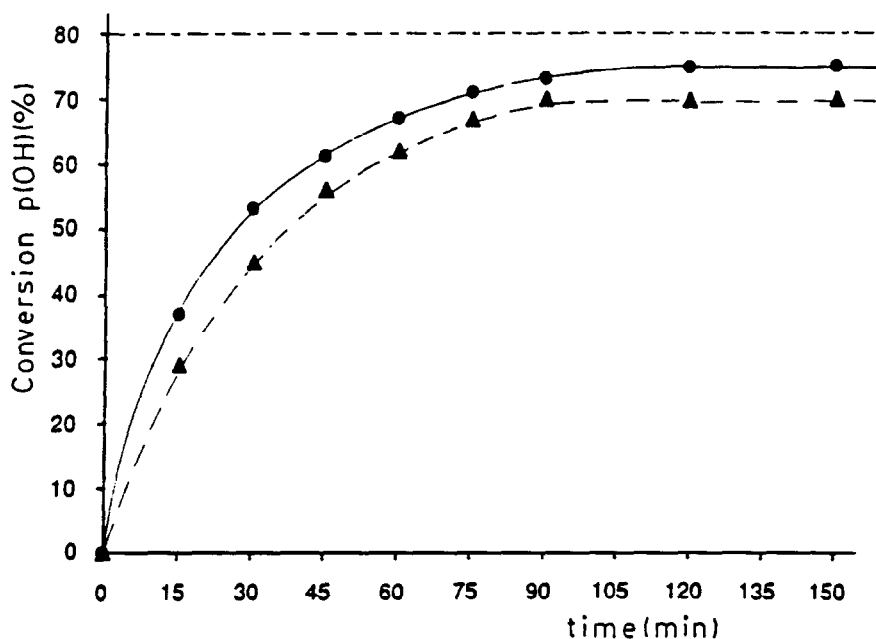**Figure 5** Polyadditions in bulk of castor oil (●) and R_3G (▲) with MDI at 60°C. r = NCO/OH = 0.8. Conversion p(OH) = f (time). (————) theoretical conversion limit = 80%

same general phenomenon was observed in the bulk polyadditions of (HTPB + HMDI or MDI)[10] and (azelaic acid + o-phthalic anhydride + trimethylol propane)[11] systems. Finally, like (HTPB + HMDI or MDI) systems[10], here the bulk polyadditions of (R_3G + MDI) do not follow second order kinetics as soon as conversions exceed 50–60%.

If the second order kinetics are considered, the calculated rate constants k equal 1.06–1.72 and 2.74 L mol^{-1} min^{-1} at 40, 50 and 60°C respectively. Finally, the Arrhenius plot gives an enthalpy of activation $\Delta H^{\ddagger}$ = 40 kJ mol^{-1}.

Effects of the nature of diisocyanates

Aliphatic isocyanates are known to be less reactive

than aromatic isocyanates[12]. The rates of reaction of R_3G with MDI, 2,6-TDI and HMDI are compared in *Figure 4*. Here again, whatever the nature of the diisocyanate may be p(OH) is limited at 70%. This limiting value is presumably due to the crosslink density presented by the CO-PUs, at least those obtained at temperature lower than 60°C.

Behaviour of castor oil (CO)

The bulk polyadditions of CO (0.7 R_3G + 0.3 R_2XG) (*Scheme 1*[1]) and R_3G with MDI at 60°C, with NCO/OH = 0.8 are compared in *Figure 5*. With 30% of diols (R_2XG), the more accessible and thus more reactive CO hydroxyls reach a higher conversion limit
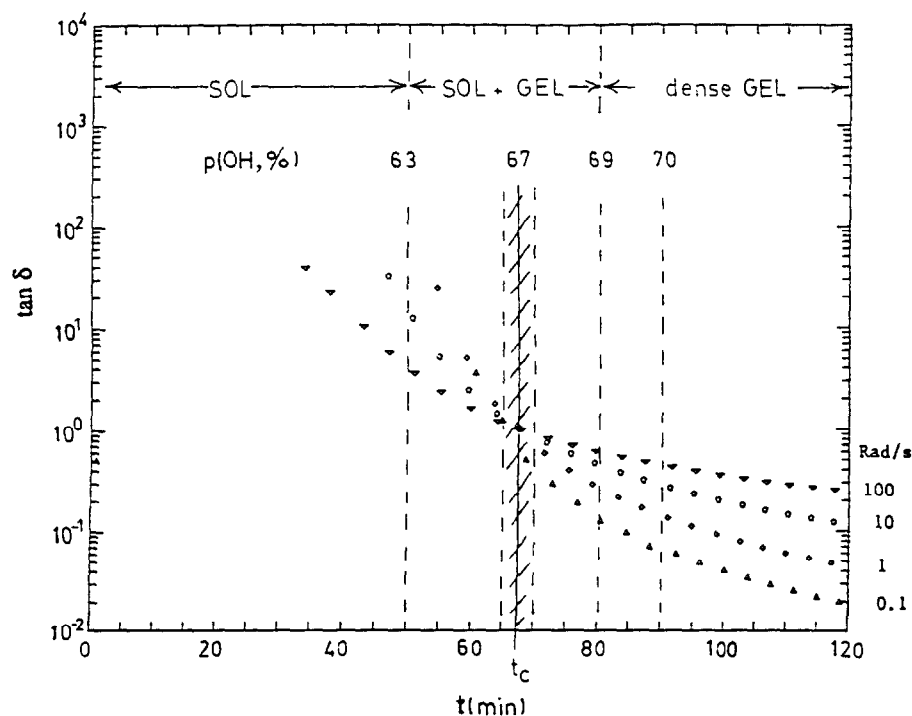
Figure 6 Loss $\tan\delta = f$ (time, min) at four angular frequencies (0.1, 1, 10, 100 rad s^{-1}). Bulk polyadditions of (R$_3$G + MDI) at 50°C with NCO/OH = 0.8

Table 1 Critical dynamic behaviour of the gelation of triricinoleate of glycerol (R$_3$G) with MDI, 2,6-TDI and HMDI (NCO/OH = 0.8). Determination of critical times (t_c) and measurements of loss tangents ($\tan\delta$) and viscoelastic exponents (Δ)

Diisocyanate	T (°C)	t_c (min)	$\tan\delta$	Δ [equation (3)]
MDI	50	67 ± 2	1.1 ± 0.1	0.53 ± 0.03
2,6-TDI	50	190 ± 2	1.7 ± 0.1	0.66 ± 0.02
HMDI	80	240 ± 2	2.0 ± 0.1	0.70 ± 0.01

(p_I). If the second order kinetics are considered, one has

$$k(\text{CO}) = 2.3 \times 10^{-2} > k(\text{R}_3\text{G})$$

$$= 1.7 \times 10^{-2}\,\text{l}\,\text{mol}^{-1}\,\text{min}^{-1}$$

and

$$p_I(\text{OH, CO}) = 75\% > p_I(\text{OH, R}_3\text{G}) = 70\%$$

or

$$p_I(\text{NCO, CO}) = 93.7\% > p_I(\text{NCO, R}_3\text{G}) = 87.5\%$$

Obviously, the higher conversion limit of CO is due to its lower crosslink density because of the presence of R$_2$XG diols as chain extenders.

Dynamic mechanical localization of the gel point (GP)

It has been suggested[13,14] that the GP or more precisely the gel time (G_t) or critical time (t_c)—time at which the sol–gel transition occurs—may be localized at the crossover point of the loss (G'') and the storage (G') moduli as measured during the cross-linking reaction time (t). At G_t, the loss tangent ($\tan\delta$) becomes independent of the frequency

$$\tan\delta = G''/G' = \tan(\Delta\Pi/2) \qquad (3)$$

Δ is the viscoelastic exponent of the frequency ω

$$G' \sim G'' \sim \omega^\Delta \qquad (4)$$

Figure 6 shows the typical variations of $\tan\delta = f(t)$ measured at four angular frequencies of the (R$_3$G + MDI) mixture at 50°C with NCO/OH = 0.8. The sol–gel transition was found at a unique crossing point. The features of the dynamic mechanical behaviour during the gelation in bulk of R$_3$G with 2,6-TDI and HMDI were similar. The results are reported in *Table 1*. In all cases, the limits of conversion determined in dense gels are slightly larger than those found at t_c. These natural conversion limits greatly facilitate obtaining gelled samples synthesized with different r (=NCO/OH) for the graphical determination of $\overline{F_w}(\text{OH})$.

In contrast with the (propylene oxide glycol + tris (4-isocyanato)thiophosphate) systems[16], the $\tan\delta$ and Δ values of the three mixtures studies here were not noticeably affected by the r (=NCO/OH) ratios. With MDI, Δ only increases from 0.5 to 0.56 when r decreases from 1 to 0.55. Actually the differences in $\tan\delta$ and Δ should depend on the natures—aliphatic or aromatic— of the diisocyanate cross-linkers incorporated. With R$_3$G, the smaller Δ is, the larger number of aromatic cycles that R$_3$G-based polyurethane has. The largest Δ value (= 0.7) is observed with the aliphatic HMDI.

Graphical determination of $\mathbf{F}_W(OH)$

The determination of $\overline{F_w}$ concerns specifically radical prepolymers.

In radical polymerization, reactive end groups may be created in three different steps: initiation, termination and chain transfer to polymer. Because of the complexity of these functionalization mechanisms, in spite of the number of published papers, if the $\overline{F_n}$s of reactive ends of the radical prepolymers may be easily determined by
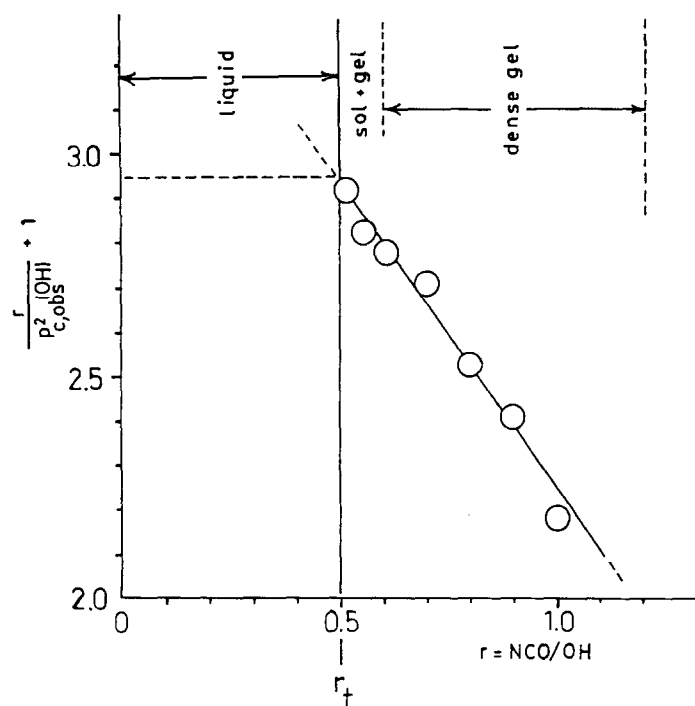
Figure 7 Bulk polyadditions of $(R_3G + MDI)$ at 50°C. Variations of $[r/p^2_{c,obs}(OH)] + 1 = f(r)$ with $r = NCO/OH$. r_t = threshold r-value. $\overline{F_w}(OH)$ $(R_3G) = F(OH)(R_3G) = 2.92 \pm 0.07$

chemical analysis combined with the measurements of their number-average molecular weights $(\overline{M_n})$, their $\overline{F_w}$s remain generally unknown. To our knowledge, there is no general method allowing the determination of $\overline{F_w}$s.

Here, thanks to the well-known $F_n(OH)$s and $F_w(OH)$s of R_3G and CO, it is possible to establish the optimal conditions needed for the graphical determination of $F_w(OH)$ by extrapolation of the linear variations of $[(r/p_c^2(OH)) + 1]$ vs r.

In the tridimensional polyaddition of R_3G (or CO) with diisocyanate (DI) with $r = NCO/OH = 0.8$, as soon as the mixture reaches its gel point $(\overline{M_w} \to \infty)$, the p_c of the minority reactive groups (NCO) is given by equation (5)[7,8]

$$rp_c^2(NCO) = [(\overline{F_w}(OH) - 1)(\overline{G_w}(NCO) - 1]^{-1}$$

$$\text{for } r = NCO/OH < 1 \tag{5}$$

$\overline{F_w}(OH) = 3$ and 2.8 for R_3G and CO respectively; $\overline{G_w}(NCO) = G(NCO) = 2$ for DI.
Hence

$$\overline{F_w}(OH) = \frac{r}{p_c^2(OH)} + 1 \quad \text{for } r > 1$$

$$\overline{F_w}(OH) = \frac{1}{rp_c^2(OH)} + 1 \quad \text{for } r > 1 \tag{6}$$

It is important to remember that equations (5) and (6) are only valid if

(a) all reactive groups of the same type (NCO or OH) are equireactive,

(b) their reactivities remain constant during the polyaddition, and

(c) there is no intramolecular reaction or cyclization.

In actuality, none of these ideal conditions is fulfilled. Nevertheless, because of the distance between OH groups, conditions (a) and (b) should be approximately

filled. However, ideal conditions may only be encountered at the very beginning of the reactions.

Experimentally, it is observed that regardless of the reaction temperature (*Figure 3*) and the nature of the diisocyanate (*Figure 4*), the reaction rate drastically decreases near the GP. At and beyond the GP, polyaddition reactions are almost stopped (*Figures 3–6*). It is thus easy to get gelled polymers with experimental p_c values somewhat larger relative to actual p_c values.

According to equations (6), in ideal conditions, with the total conversions of the minority reactive groups (NCO or OH for $r < 1$ or $r > 1$ respectively), gelation will occur in the intervals

$$0.5 \le r \le 2 \quad \text{for } R_3G[F(OH) = 3]$$

and

$$0.55 \le r \le 1.8 \quad \text{for } CO[\overline{F_w}(OH) = 2.8]$$

Because of the defectiveness (waste of reactive groups due to cyclization, etc.) of the bulk polyadditions, observed critical conversions $[p_{c,obs}(OH)]$ are always larger than those calculated $[p_{c,calc}(OH)]$ using equation (5). The near the r-value is to unity, the larger the differences $\Delta p_c(OH)$ $(= p_{c,obs}(OH) - p_{c,calc}(OH))$ are. For R_3G as for CO, $\Delta p_c(OH)$ increases from 1–2% to a maximum of 20% for r increasing from near r_t (threshold r-value) to around 1 respectively.

It is reasonable to assume that because the crosslink density is maximum around $r = 1$, $\Delta p_c(OH)$ reaches its largest value.

$p_{c,obs}(OH)$s being larger than $p_{c,calc}(OH)$s, according to equation (6), to each couple of $[r, p_{c,obs}(OH)]$ values corresponds an apparent functionality $\overline{F_{w,a}}(OH)$ smaller than the actual $\overline{F_w}(OH)$. Thus $\overline{F_w}(OH)$ cannot be directly calculated from equation (6) under any circumstances. Moreover, when the presence of gel is visually observed (dissolution test), the mixture is already beyond its gel point.
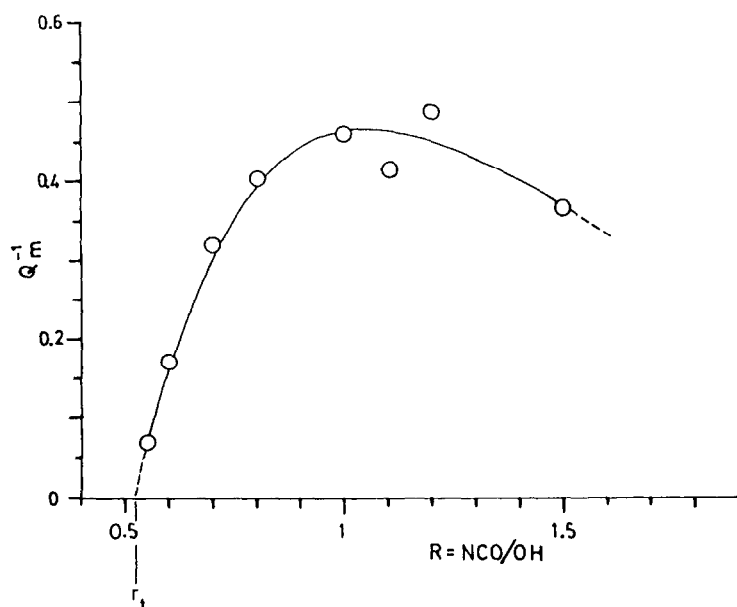
Figure 8 Bulk polyadditions of (R_3G + MDI) at 50°C. Variations of $Q_m^{-1} = f(r)$ with r = NCO/OH. r_t = threshold r-value

It is instructive to note that Δp_c(OH) tends to zero when r is near its lower limit. Thus, the principle of the graphical determination of $\overline{F_w}$(OH) proposed here is based on the extrapolation of the linear variations of $\overline{F_{w,a}}$(OH) $[= (r/p_{c,obs}^2$(OH)) + 1]$ as a function of r to the threshold r-value r_t ($= 0.5$ and 0.55 for R_3G and CO respectively) at which point critical gels should be formed. At r_t, Δp_c(OH) is expected to be zero and $\overline{F_w}$(OH) should reach its actual value.

The typical variations of $\overline{F_{w,a}}$(OH) vs r in the $0.5 \leq r \leq 1$ region for (R_3G + MDI) at 50°C are illustrated in *Figure 7*. The extrapolated value of $\overline{F_w}$(OH) is found at the intersection of $\overline{F_{w,a}}$(OH) with the vertical $r_t = 0.5$. In spite of some uncertainty as to the actual r_t value, and consequently those of p_c(OH)s, the extrapolations give

$$2.9 \leq \overline{F_w}(OH)(R_3G) = F(OH)(R_3G) \leq 3$$

and

$$2.7 \leq \overline{F_w}(OH)(CO) \leq 2.8$$

in good agreement with the theoretical $\overline{F_w}$(OH) values of 3 and 2.8 for R_3G and CO respectively. The relative error is only around 2%.

Swelling at equilibrium

The extent of the maximum swelling ratio Q_m is inversely proportional to the density of crosslinks in the gel networks[14,15,17].

$$Q_m = V_m/V_o \qquad (7)$$

V_m is the volume of the swollen gel and V_o, that of the dry extracted gel.

At the percolation threshold or for the least cross-linked gel, V_o tends to zero and Q_m, to infinity ($Q_m \to \infty$). Thus the extrapolation of $Q_m^{-1} = f(r)$ to zero permits another estimation of the threshold r-value r_t. The variations of Q_m^{-1} vs r are illustrated in *Figure 8*. It is informative to note that in the $1 \leq r \leq 1.1$ region, Q_m is minimal, which corresponds to the largest crosslink density. Extrapolations to $Q_m^{-1} = 0$ give the threshold values $0.50 \leq r_t \leq 0.54$ and $0.55 \leq r_t \leq 0.60$ for R_3G

and CO respectively. In these r-regions, the consumption of NCO groups was found to be complete. Thus according to equations (2) and (6), one has

$$2.85 \leq \overline{F_w}(OH, R_3G) \leq 3$$

and $$2.67 \leq \overline{F_w}(OH, CO) \leq 2.82$$

in good agreement with the $\overline{F_w}$(OH)s obtained by extrapolation of $\overline{F_{w,a}}$(OH) $= f(r)$ (*Figure 7*).

ACKNOWLEDGEMENTS

REFERENCES

1. Tran, Ng. B., Vialle, J. and Pham, Q. T., *Polymer*, 1997, **38**, 2467.
2. Petrovic, Z. S. and Fajnik, D., *J. Appl. Polym. Sci.* 1984, **29**, 1031.
3. Saxena, P. K., Srnivasan, S. R., Rouz, J. H. and Ilavsky, M. I., *J. Appl. Polym. Sci.*, 1992, **44**, 1343.
4. Suresh, K. I. and Thachil, E. T., *Angew. Makromol. Chem.*, 1994, **218**, 127.
5. Homan, J. G., Yu, X. H., Connor, T. J. and Cooper, S. L., *J. Appl. Polym. Sci.*, 1991, **43**, 2249.
6. Suthar, B., Dave, M. and Jadav, K., *J. Appl. Polym. Sci.*, 1993, **50**, 2143.
7. Stockmcycr, W. H., *J. Polym. Sci.*, 1952, **9**, 69; 1953, **12**, 125.
8. Macosko, C. W. and Miller, D. R., *Macromolecules*, 1976, **9**, 199.
9. Allard-Breton, B., Audenaert, M. and Pham, Q. T., *Macromol. Chem. Phys.*, 1996, **197**, 1651.
10. Descheres, I. and Pham, Q. T., *Makromol. Chem.*, 1990, **191**, 891.
11. Petiaud, R., Waton, H., Coyard, H. and Pham, Q. T., *Polymer*, 1992, **33**, 5056.
12. Descheres, I. and Pham, Q. T., *Makromol. Chem.*, 1986, **187**, 1963.
13. Chambon, F. and Winter, H. H., *J. Rheology*, 1987, **31**, 683.
14. Chambon, F., Petrovic, Z. S., Macknight, W. J. and Winter, H. H., *Macromolecules*, 1986, **19**, 2146.
15. Cohen-Addad, J. P. and Girard, O., *Macromolecules*, 1992, **25**, 593.
16. Winter, H. H., Morganelli, R. and Chambon, F., *Macromolecules*, 1988, **21**, 532.
17. Harrison, D. J. P., Yates, W. R. and Johnson, J. F., *J. Macromol. Sci.-Rev. Macromol. Chem. Phys.*, 1985, **C25**, 481.